J. W. Edington and M. J. Klein

understood when the form of a jog in a Frank sessile dislocation is taken into account. Both the Frank sessile dislocation and the jog are parallel to ⟨110⟩ directions and thus, when the jog reaches the corner of the triangle it disappears. Accordingly it is reasonable that, under conditions of flow of vacancies through the lattice towards one particular edge of a triangle, the dislocation at that edge may climb to produce a distorted triangle like that in Fig. 2(a).

There is a close morphological relationship between the "A" and "B" defects described above. Therefore any process which explains the formation of "A" defects should also be applicable to the formation of the "B" defects. The possibility that a pair of "A" defects could have grown together to form the "B" defects in Figs. 1 and 2 cannot be completely ruled out. However, even in large clusters of closely spaced Frank sessile loops, the growth of loops together in the same plane has never been observed by the present authors. Therefore such an event between the relatively uncommon "A" defects is considered to be extremely unlikely.

The formation of "A" defects can be described in terms of the complex collapse of an ellipsoidal vacancy cluster to produce a small defect of special structure which could subsequently grow to form the observed two-layer loop. However this description is difficult to apply to the "B" defect in Fig. 1 because the centers of the two triangles are approximately 1500 Å apart, and the minimum diameter of the ellipsoid before collapse would therefore be approximately 1500 Å. The occurrence of such three-dimensional vacancy clusters is unlikely because their diameter is between three and five times greater than the largest voids previously observed[4,5] in quenched aluminum.

An alternative description of the formation of the "A" defect is one which allows for the formation of the triangular Frank sessile loop on a growing Frank loop. Such an explanation could be based on the nucleation of the first, and subsequently the second, Frank sessile loop on a persistent lattice inhomogeneity which attracts vacancies. However this mechanism would not explain either the occurrence of the "B" defect, nor that of the "A" defects which have single triangles near the edge of an equal-sided hexagon.[2,6] A more reasonable mechanism would involve the existence of a high local concentration of vacancies in the vicinity of the stacking fault of a growing Frank loop. Under these conditions, new Frank sessile dislocation loops will be nucleated near the pre-existing faulted loop. Such a locally high vacancy concentration could be the result of the domination of any attractive force which exists between the vacancies and the stacking fault over the hydrostatic stress field of the Frank sessile dislocation which drives vacancies away from the center of the loop.[7] Using this approach, the fact that not every Frank loop contains an inner triangle probably reflects the statistical chance of the occurrence of the necessary vacancy interactions which are required to form a nucleus that is capable of growing. Not only is this latter mode of formation of "A" defects consistent with the quenching conditions which favored their formation, but it is also consistent with their distribution in the specimen as pointed out by Shimomura and Yoshida.[6] It is also consistent with the occasional noncentrally located triangle[2,6] and the observed growth of the triangle at the expense of the hexagon.[8] It is therefore concluded that successive nucleation of new Frank loops on growing Frank loops is the most reasonable explanation of the formation of both "A"- and "B"-type defects.

[1] S. Yoshida and Y. Shimomura, J. Phys. Soc. Japan 18, 1590 (1963).
[2] J. W. Edington and R. E. Smallman, Phil. Mag. 11, 1109 (1965).
[3] S. Yoshida, M. Kiritani, and Y. Shimomura, International Conference on Lattice Defects in Quenched Metals, 1964 (Academic Press Inc., New York, 1965), p. 713.
[4] M. Kiritani, Y. Shimomura, and S. Yoshida, J. Phys. Soc. Japan 19, 1624 (1964).
[5] G. Das and J. Washburn, Phil. Mag. 11, 955 (1965).
[6] Y. Shimomura and S. Yoshida, J. Phys. Soc. Japan 20, 1667 (1965).
[7] M. J. Whelan, and R. M. J. Cotterill, reported by R. M. J. Cotterill, Ref. 3, p. 351.
[8] Y. Shimomura, J. Phys. Soc. Japan 20, 965 (1965).

Slip and Fracture in Single Crystals of Thoria

J. W. Edington and M. J. Klein
*Metal Science Group, Battelle Memorial Institute, Columbus Laboratories, Columbus, Ohio*
(Received 14 March 1966; in final form 30 March 1966)

VERY little is known about the deformation modes of thoria. Gilbert[1] has shown that fracture can occur on {111} planes, and at elevated temperatures slip takes place on {110} and {111} planes in small particles of thoria embedded in tungsten. However, these particles were subject to a strong hydrostatic stress component during deformation, and their behavior need not be typical of that of the bulk material. It has also been reported[2] that the fracture plane in single crystals of thoria is {100}. This note describes a preliminary investigation of both the slip and fracture modes in single crystals of thoria using etch pit and transmission electron microscopy techniques.

Single crystals of thoria were purchased from the Norton Company, Ontario, Canada. Spectrographic and gravimetric analysis showed the impurity levels given in Table I. The elements Mg, Cr, Sn, Pb, W, Na, V, Nb, Mo, Zn, Ti, Co, B, and Al were not detected.

TABLE I. Impurity levels in as-received ThO_2.

Impurity Weight%	Si	Fe	Cu	Ni	Ca	C	N_2
	<0.01	<0.01	0.02	<0.01	0.01	0.0014	<0.001
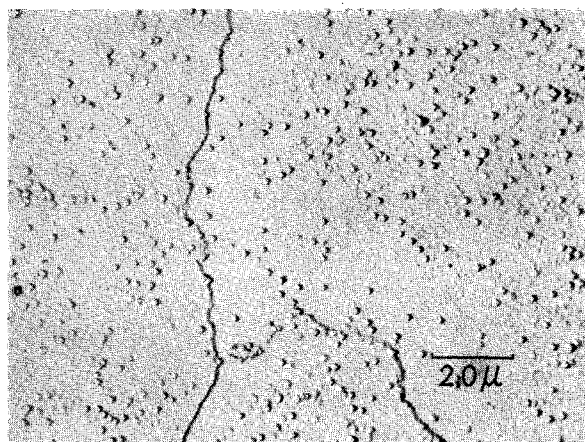
(a)
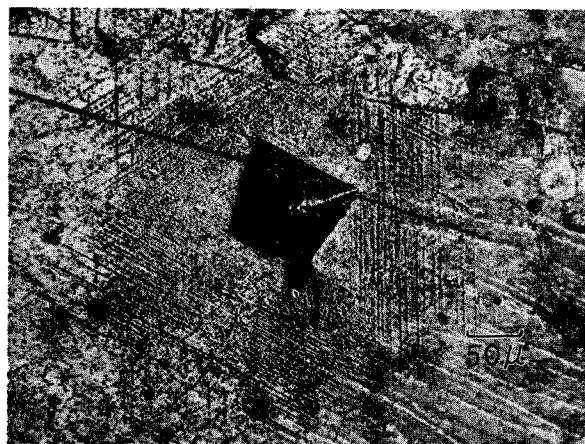
(b)

FIG. 1. (a) Dislocation arrangement on a cleavage face after annealing at 1250°C for 1 h, as revealed by etch pits. (b) Slip lines around a hardness impression made at 900°C on a cleaved surface, as revealed by etching.

FIG. 2. Matching of slip lines across two intersecting {111} cleavage planes A and B.

Flat surfaces suitable for slip line determinations were obtained by cleaving single crystals. The cleavage plane was identified as {111} by Laué back reflection techniques in agreement with the results of Gilbert.[1] Hot hardness impressions were made on {111} faces of cleaved disks, and the geometry of slip around these impressions was studied. For additional slip studies cleaved crystals, 0.5×0.5×0.8 cm were compressed in an Instron testing machine at a strain rate of 10^{-2} sec^{-1}. All crystals were annealed in air at 1250°C for one hour prior to testing. In order to facilitate studies of slip modes, an etching procedure was developed for revealing dislocations on {111} faces. The treatment requires the crystal to be immersed in boiling ammonium fluoride for five minutes. Triangular etch pits whose sides are parallel to the intersection of {111} planes with cleavage faces are produced at dislocations. Figure 1(a) shows a typical etch-pitted {111} cleavage face which exhibits single dislocations and low-angle boundaries after the annealing treatment given before deformation. The dislocation density in such a heat-treated crystal is approximately 3×10^6 cm^{-2}.

Slip lines and dislocation etch pits were observed around hardness indentations made from room temperature up to 900°C. These slip lines intersected the {111} cleavage surface along $\langle 110 \rangle$ directions, as shown in Fig. 1(b). However, {100}, {111}, and some {110} slip planes intersect {111} faces along $\langle 110 \rangle$ directions. It is therefore necessary to carry out a two-surface analysis to determine the slip plane. Such an analysis has been performed on {111} faces intersecting at 70° for a specimen deformed in an Instron testing machine to 1% ϵ at 900°C. As shown in Fig. 2, the slip lines on adjacent {111} faces are parallel if these faces

are rotated about their zone axis until they lie in a coincident plane. This behavior is only consistent with slip on {100} planes.

Since thoria has the calcium fluoride structure, the anticipated Burgers vector for dislocations is $\frac{1}{2}a\langle 110 \rangle$, the shortest repeat distance. To determine the Burgers vector of dislocations in this material, thin foils, produced by cleavage, were examined in the electron microscope. The dislocation density in these foils was low although occasionally hexagonal networks were observed. However, none of these networks showed extension of the dislocation nodes. Occasionally slip bands like that in Fig. 3(a) were observed. Frequently such bands, whose slip plane is always {100}, originate at small cracks existing at the edge of the thin foil. It is believed that these dislocation bands are introduced during cleavage. The dislocations shown in Fig. 3(a) were observed to be invisible under a $2\bar{2}0$ reflection [see Fig. 3(b)] but visible under $3\bar{1}\bar{1}$, $\bar{1}\bar{1}1$, $0\bar{2}2$, $\bar{2}02$, $\bar{3}20$, and $2\bar{1}1$ reflections. On the basis of the observed electron contrast behavior, it can be concluded that the Burgers vector of the dislocations must be either $\frac{1}{2}a[110]$ or $\frac{1}{6}a[\bar{1}12]$. Although Ashbee[3] has pointed out that dislocations with Burgers vector $\frac{1}{6}a\langle 112 \rangle$ can exist in urania, which is isostructual with thoria, such dislocations would have associated stacking faults. However, the present observations failed to show stacking-fault fringes, and it is therefore concluded that the Burgers vector of these dislocations is $\frac{1}{2}a[110]$.

To summarize: Hardness impressions have been made on {111} faces of single crystal specimens of thoria in the temperature range room temperature to 900°C. Etch-pit studies of slip lines formed around these impressions are consistent with slip on {100} planes.
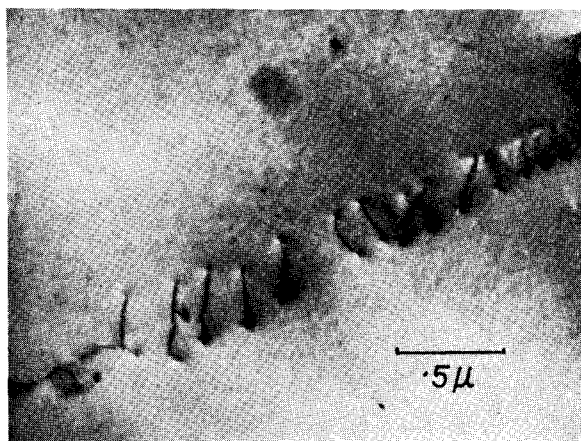
(a)
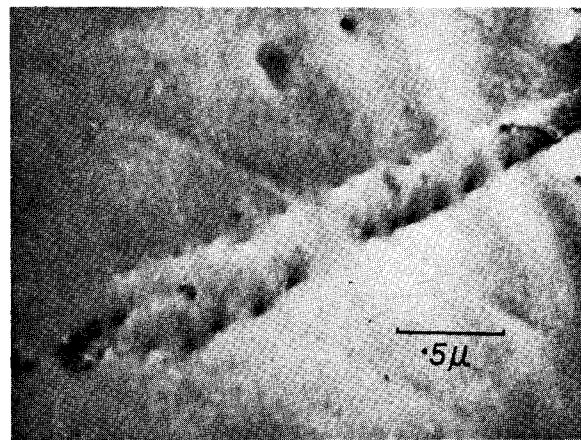
(b)

FIG. 3. (a) A dislocation array originating at the edge of a cleaved foil. The slip plane is (001), g is $0\bar{2}2$. (b) The area shown in Fig. 3(a), $g=2\bar{2}0$ and the dislocations are out of contrast.

This slip plane has been positively identified by etch-pit studies of adjoining {111} faces of single crystals deformed at 900°C, and also by transmission electron microscopy studies of foils cleaved at room temperature. The fracture plane at room temperature and 900°C has been identified as {111}.

The authors would like to thank R. F. Blake of the Norton Company for supplying the crystals and J. W. Sheckherd for his help with the experimental work. The financial support of this work by Battelle Memorial Institute is also gratefully acknowledged.

[1] A. Gilbert, Phil. Mag. **12**, 139 (1965).
[2] W. B. Campbell, V. J. Hurst, and W. E. Moody, J. Am. Ceram. Soc. **42**, 262 (1959).
[3] K. H. G. Ashbee, Proc. Roy. Soc. (London) **A280**, 37 (1964).

Comments on the Junction Boundary Conditions for Heterojunctions

L. L. CHANG

IBM Watson Research Center, Yorktown Heights, New York

(8 February 1966)

IN a recent article, Chang[1] applied the general boundary conditions obtained for homojunctions by Fletcher[2] to heterojunctions, and concluded from the analyses that the two band discontinuities were equal except for the correction of about kT/q. This conclusion is in direct contrast to that derived from the Anderson model.[3] Since the band discontinuity is the very fundamental concept in heterojunction physics, we feel it important to clarify the situation.

We consider, to be specific, an n (narrow gap)–p (wide gap) heterojunction in the absence of degeneracy and surface effects. The energy levels at thermal equilibrium are shown in Fig. 1, where ψ is the electrostatic potential and $\chi+\phi_n$ the chemical potential with χ being the electron affinity. D_c and D_v are the discontinuities of the conduction and valence band edges, respectively. The Fermi level E_f is constant throughout the structure so that

$$d\psi/dx + d(\chi+\phi_n)/dx = 0. \quad (1)$$

The current can be obtained by multiplying Eq. (1) by the electronic charge, the carrier concentration, and mobility. The first term, then, gives the field current. The second term gives what may be considered the generalized diffusion current, since the chemical potential is actually the driving force for diffusion. Therefore, thermal equilibrium may be regarded as resulting from the mutual compensation of field and diffusion current components even in the case where χ is not a constant such as that at the interface of a heterojunction. In regions 1 and 2 of Fig. 1, where χ does not vary in space, the second term in Eq. (1) reduces to $d\phi_n/dx$, which can be shown to be proportional to the concentration gradient and gives the usual diffusion current. The diffusion potential V_d, being equal to the sum of the partial potentials that exist in the two regions $V_{d1}+V_{d2}$, can be found readily

$$V_d = \frac{kT}{2q}\left(\ln\frac{n_1p_2}{p_1n_2} + \ln\frac{p_{10}n_{20}}{n_{10}p_{20}}\right). \quad (2)$$
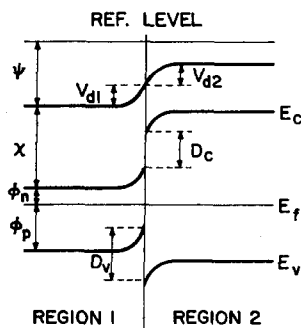
REF. LEVEL

FIG. 1. The energy band diagram of an n–p heterojunction at equilibrium.

Subscripts 1 and 2 refer to quantities in the bulk of the semiconductors 1 and 2, respectively. The second subscript zero is used to denote quantities at the interface.

When a bias is applied to the heterojunction, the injection relations can be written down in analogy with the homojunction under the assumptions of long carrier diffusion length and quasi-equilibrium state.[1] δ_1 and δ_2, the injection carrier concentrations in the two regions, can then be solved

$$\delta_1 = p_1(e^{qV/kT}-1)\left(1+\frac{n_2}{p_2}e^{qV/kT}\right)\left(1-\frac{p_1n_2}{n_1p_2}e^{2qV/kT}\right)^{-1}$$

$$\delta_2 = n_2(e^{qV/kT}-1)\left(1+\frac{p_1}{n_1}e^{qV/kT}\right)\left(1-\frac{p_1n_2}{n_1p_2}e^{2qV/kT}\right)^{-1}. \quad (3)$$

From the last term in Eq. (3), Chang defined a barrier potential by $(kT/2q)\ln(n_1p_2/p_1n_2)$ and identified it with V_d as shown in Fig. 1. This procedure is not justified. A comparison of such a definition with Eq. (2) shows that the second term in the equation is forced to vanish. Since, by neglecting a term of the order of kT/q involving the effective masses, we can express

$$\ln(p_{10}n_{20}/n_{10}p_{20}) = (q/kT)(D_v-D_c), \quad (4)$$

it is not surprising that Chang obtained the result of equal band discontinuities. If the correct expression of V_d, Eq. (2), is substituted into Eq. (7) of Ref. 1, two identical equations result as expected from which the band discontinuities cannot be solved. From Fig. 1 it is seen that the discontinuities can be related to the electron affinities and energy gaps by $D_c=\chi_1-\chi_2$, $D_v = (E_{g2}-E_{g1})+(\chi_2-\chi_1)$ as originally proposed.[3]

It should be mentioned that the injection relations may or may not govern the electron conduction in a heterojunction. In addition to the recombination in the junction region, other effects such as interface states and tunneling may become important and the possibility of a rectifying n–n or p–p heterojunction exists. However, the expressions relating the band discontinuities to the electron affinities and energy gaps are still valid in the existence of surface states, if now the electron affinities are so defined to take these states into account.

[1] Y. F. Chang, J. Appl. Phys. **36**, 3350 (1965).
[2] N. H. Fletcher, J. Electron. **2**, 610 (1957).
[3] R. L. Anderson, Solid State Electron. **5**, 341 (1962).

Heterojunction Boundary Conditions

T. L. TANSLEY

Mullard Research Laboratories, Redhill, Surrey, England

(Received 21 February 1966)

A RECENT communication by Chang[1] involves assumptions which are inappropriate to the analysis of heterojunction boundary conditions. Accepting the formal values of the injected carrier concentrations δ_1 and δ_2 appearing in Eqs. (4) and (5), then their assumed equivalence to those of the homojunction case, written as Eq. (7), requires the band edge discontinuities D_v and D_c to vanish.

For a more detailed discussion of the conditions we begin at Chang's Eq. (5). Injected carrier concentrations are dependent upon both the curvature of the bands and their total displacements. In the homojunction case, the curvature and displacement are uniquely related and no discontinuity in the bands arises. Indeed, it may be possible to define the barrier potential of the heterojunction in this way, but we can go no further. Certainly we cannot assume this "barrier potential" to be the sum of the diffusion voltages appearing in the respective materials [Eqs. (6) and (7)] as the band discontinuities, normal in heterojunctions, form the critical part of the band displacements and thereby play a large part in determining the injected carrier concentrations. The equivalence assumed by Chang can only obtain in the singular case of conduction and valence band discontinuities being zero.

[1] Y. F. Chang, J. Appl. Phys. **36**, 3350 (1965).